



Deposited via The University of Leeds.

White Rose Research Online URL for this paper:

<https://eprints.whiterose.ac.uk/id/eprint/154859/>

Version: Accepted Version

Proceedings Paper:

Zeb, S, Abbas, Q, Hassan, SA et al. (2019) NOMA Enhanced Backscatter Communication for Green IoT Networks. In: Proceedings of the International Symposium on Wireless Communication Systems. International Symposium on Wireless Communication Systems (ISWCS) 2019, 27-30 Aug 2019, Oulu, Finland. , pp. 640-644. ISBN: 9781728125275. ISSN: 2154-0217. EISSN: 2154-0225.

<https://doi.org/10.1109/ISWCS.2019.8877102>

© 2019 IEEE. Personal use of this material is permitted. Permission from IEEE must be obtained for all other uses, in any current or future media, including reprinting/republishing this material for advertising or promotional purposes, creating new collective works, for resale or redistribution to servers or lists, or reuse of any copyrighted component of this work in other works.

Reuse

Items deposited in White Rose Research Online are protected by copyright, with all rights reserved unless indicated otherwise. They may be downloaded and/or printed for private study, or other acts as permitted by national copyright laws. The publisher or other rights holders may allow further reproduction and re-use of the full text version. This is indicated by the licence information on the White Rose Research Online record for the item.

Takedown

If you consider content in White Rose Research Online to be in breach of UK law, please notify us by emailing eprints@whiterose.ac.uk including the URL of the record and the reason for the withdrawal request.

NOMA Enhanced Backscatter Communication for Green IoT Networks

Shah Zeb*, Qamar Abbas*, Syed Ali Hassan*, Aamir Mahmood[‡], Rafia Mumtaz*, S. M. Hassan Zaidi*,
Syed Ali Raza Zaidi[†], and Mikael Gidlund[‡]

*School of Electrical Engineering & Computer Science (SEECS),
National University of Sciences & Technology (NUST), Pakistan.

[†] School of Electronic and Electrical Engineering, The University of Leeds, Leeds, UK.

[‡]Department of Information Systems & Technology, Mid Sweden University, Sweden.

Email: *{szeb.msee17seecs, qabbas.phdee17seecs, ali.hassan, rafia.mumtaz, drzaidi}@seecs.edu.pk,

[‡]{firstname.lastname}@miun.se, [†]s.a.zaidi@leeds.ac.uk

Abstract—Backscatter communication has recently emerged as a promising technology to enable the passive sensing-based Internet-of-things (IoT) applications. In a backscatter communication network, uplink transmissions of multiple nodes are usually multiplexed in time- or frequency-domain to avoid collisions, yet it is desirable to improve the uplink capacity further. In this paper, we study a wireless-powered backscatter communication system, where the sensors use a hybrid channel access scheme by combining time division multiplexing access (TDMA) with power-domain non-orthogonal multiple access (PD-NOMA) to enhance the system performance in terms of outage probability and throughput. Our analysis shows that the proposed PD-NOMA increases both the spectrum efficiency and the throughput of the system.

Index Terms—Backscatter communication, Internet-of-things (IoT), non-orthogonal multiple access (NOMA), wireless-powered communication.

I. INTRODUCTION

The Internet-of-things (IoT) is anticipated to connect billions of sensors/devices to bring digital transformation in an extensive range of applications such as agriculture, industries, healthcare, and homes [1]. For instance, in the process industry, an IoT network comprised of wireless sensor networks (WSNs) and radio-frequency identification (RFID) can be used to build an automated system to track and monitor the production chain and quality [2]. Similarly, in smart agriculture, such an IoT network can monitor water absorbed by crops, pest control mechanism for plants, and the use of fertilizers to maximize the yield.

However, for efficient data aggregation from a massive number of devices, several design issues affect network performance in terms of scalability and energy efficiency [3]. In an IoT network, typically, resource-constrained end devices communicate with central gateway or access point, which provides a centralized control over end devices through the Internet. Therein, the gateway must ensure energy- and spectral-efficient medium access opportunities for an increasing number of devices with minimal collisions. Recently in the literature, a great deal of attention is focused on energy-efficient *green communication* in IoT networks.

A key aspect of green networks is the provisioning of harvested energy. For green IoT networks, wirelessly powering and energy harvesting-based approach is proposed in [4]. In wireless powered communication networks (WPCN), power is transmitted to IoT devices through radio frequency (RF) signals. One of the key enabler techniques in WPCN is backscatter communication (BackCom) [5]. A BackCom system is composed of backscatter nodes (BNs) and a reader. The reader transmits a single-tone sinusoidal RF signal. A BN doesn't have any active RF component for transmitting its sensed data. Instead, BN on receiving a reader RF signal, reflects it back to the reader. The reflection of RF signal is done through intentional impedance mismatching at the antenna input side [6]. The data is encoded over incident wave using a variation of reflection coefficients, which is achieved through varying the impedance at antenna inputs and BNs can harvest the energy as well. This principle makes the backscatter communication a prime candidate for green IoT networks.

In a BackCom system, the reader may receive reflected signals from multiple BNs during the uplink data transmission. This causes collisions/interference in uplink data transmissions at the receiver [7]. In such an event of data loss due to the collision, it has to be re-transmitted, thereby affecting the energy efficiency of BackCom-aided IoT system. An efficient multiple access scheme is, therefore, needed to multiplex multiple BNs simultaneously and reduce interference in the uplink transmissions. The authors in [8] and [9] used frequency division multiplexing (FDM) and time division multiplexing (TDM)-based access scheme for a BackCom system. Besides frequency and time multiplexing, to increase the spectrum efficiency of BackCom system, the benefits of non-orthogonal multiple access (NOMA) can be reaped if appropriately used. NOMA, by enabling several users or devices to share the same time-frequency resource block, is anticipated to be a key technology for next-generation wireless networks [10].

In this paper, NOMA-enhanced backscatter communication is considered for IoT sensors in an application-specific field. The field can be an agricultural farm or an industrial floor. Sensors use a hybrid TDMA scheme with PD-NOMA for

uplink data transmission. We use a power division-based design guidelines from [11] to realize NOMA in our BackCom system. The proposed scheme increases the spectrum efficiency and reduces collisions among the sensors. The main contributions of this paper are the followings.

- From green IoT perspective, we propose to use wireless powered communication paradigm, i.e., backscatter communication in a field of IoT sensors and use a hybrid TDMA-based PD-NOMA scheme to increase the spectrum efficiency of the system.
- The system performance analysis shows that the proposed hybrid multiplexing scheme outperforms the standalone TDMA scheme and increases the system throughput.

In the following sections, BackCom system model for a sensors network is presented and a PD-NOMA model and its analysis is discussed, which is followed by simulation results and conclusions.

II. BACKCOM SYSTEM MODEL

A. Sensor Field Model

Consider a sensor field where K IoT sensors are deployed to carry out application-specific sensing tasks. To enhance energy efficiency of the network, we assume a monostatic backscatter communication model. The monostatic backscatter architecture is composed of two components; the reader and the backscatter nodes (BNs). Let $\mathbb{K} = \{1, 2, 3, \dots, K\}$ be the set of all BNs or sensors randomly distributed in the field and let the locations of all the sensors are modeled as a Binomial point process, i.e., they are independent and identically distributed (i.i.d.) for a given coverage zone of radius R and the number of nodes in the zone is fixed. The reader transmits the power using continuous carrier waves (CW) to the sensors located inside the reader coverage zone. The coverage region for the reader is anticipated to be annular and specified by the outer radius R . As shown in Fig. 1, all sensors which are included in the reader coverage zone can backscatter the incident waves to transmit data. A BN has the following components: receiver, transmitter, microcontroller, variable impedance, energy harvester module, and information decoder. We assume that the energy harvester module in each k -th BN, $k \in \mathbb{K}$, has large battery storage, where the energy can be utilized to preserve the normal operation of sensors in long term for field use. Each BN has a distinct identification (ID) information value, which is already known to the reader.

Let $\mathbb{L} = \{1, 2, 3, \dots, L\}$ be a set of sensors which reside inside the reader coverage, where $\mathbb{L} \subseteq \mathbb{K}$. Without the loss of generality, we consider that sensor 1 is nearest to the reader and sensor L is at the farthest distance from the reader. The reader on receiving the backscattered signals from L BNs can transmit the decoded data to a cellular base station (BS). The coverage region of a reader in BackCom system is comparatively small. The successful BNs are generally closer to the reader and have a strong line-of-sight (LOS) link. Therefore, we assume a path loss-only wireless channel model

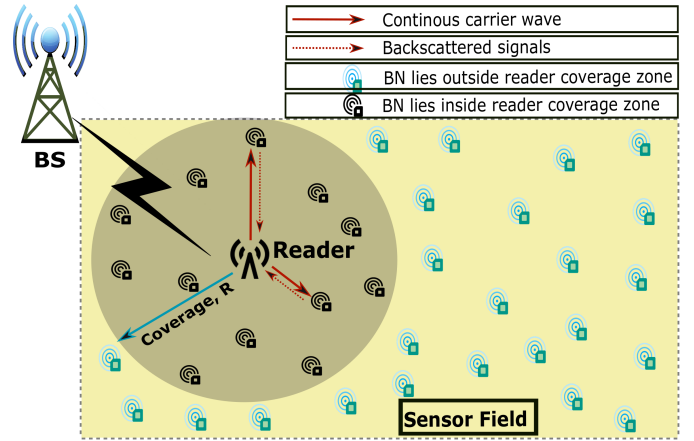


Fig. 1. Illustration of system model for K sensors deployed in field

in this study. For each l -th BN, where $l \in \mathbb{L}$, the received power, Ω_l , is given by

$$\Omega_l = \Omega_t h_l, \quad (1)$$

where Ω_t is the transmit power of the reader and h_l is the channel gain of l -th BN from the reader, which is given by

$$h_l = r_l^{-\gamma}, \quad (2)$$

where r_l is the distance between the reader and sensor l , and γ is the path-loss exponent. Each BN is characterized by two states: waiting and backscattering. In the *waiting state*, a sensor does not perform backscatter communication with the reader, rather it harvests energy from the incident continuous CW. In the *backscattering state*, the BN transmitter performs backscatter communication with the reader and it transmits the modulated signal to the reader using load or backscatter modulation. Load modulation is done by switching between the impedance states. This switching function is performed by the inbuilt microcontroller of the sensor device and it causes the change in multiple antenna-load system reflection coefficients, Γ_i , which results in backscattering [12]. The reflection coefficients are given by

$$\Gamma_i = \frac{(Z_i - Z_{\text{ant}}^*)}{(Z_i + Z_{\text{ant}}^*)}, \quad i = \{1, 2, 3, \dots, M\} \quad (3)$$

where i is an integer set, M is the total number of antenna termination impedance inside the BN, Z_i is the antenna termination impedance and Z_{ant}^* is the complex antenna impedance. We consider a binary phase shift keying (BPSK) modulation scheme for this study, i.e., $M = 2$. This results in switching between two reflection coefficients, Γ_1 and Γ_2 for each sensor. Using the assumed path-loss model, the backscattered power, Ω_{T_l} , for the l -th BN is given by

$$\Omega_{T_l} = \Gamma_i \Omega_l = \Gamma_i (\Omega_t r_l^{-\gamma}), \quad 0 \leq \Gamma_i \leq 1 \quad (4)$$

III. POWER-DOMAIN NOMA MODEL

In this section, the main focus is on the uplink communication, and we employ the hybrid TDMA scheme with PD-NOMA for the BackCom system. Without loss of generality,

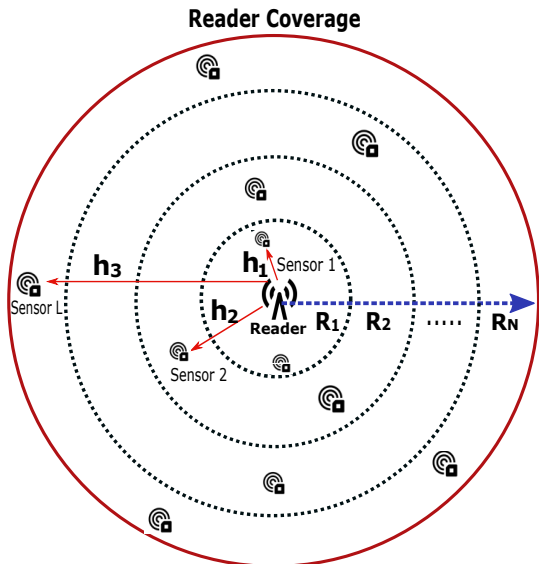


Fig. 2. Illustration of PD-NOMA model for L BNs with N subregions

we assume that distance of the first sensor from the reader is smallest and has a channel gain, h_1 , which is strongest among all sensors, whereas, the farthest user has the weakest channel gain h_L , due to the larger distance from the reader. Hence, the channel coefficients of sensors from \mathbb{L} can be assumed in ascending order as $h_1 \geq h_2 \geq \dots h_L$. In an orthogonal multiple access (OMA)-based TDMA scheme, a timeslot of T seconds is divided into multiple mini-timeslots and each sensor node is assigned a single mini-timeslot to transmit its data. To implement NOMA in the sensor network, multiple sensors are multiplexed together in a single mini-timeslot of T seconds based on large channel gain difference among them. The length of each mini-timeslot depends on the multiplexing scenario, e.g., with only TDMA scheme, duration of the single mini-timeslot is T/L seconds.

We use a region division-based approach to implement the proposed PD-NOMA. In the region division method, the reader splits the annular coverage zone into N number of virtual subregions. Let $\mathbb{R} = \{R_1, R_2, \dots, R_N\}$ be the set of new subregions formed, as shown in Fig. 2. The sensors residing in a separate N subregions are utilized for power-domain multiplexing. The reader randomly picks a sensor from each n -th subregion to implement NOMA in a single mini-timeslot unit, where $n \in \{1, 2, \dots, N\}$. The selected sensors backscatter the received signal power from the reader at different power levels. The sensors not selected for transmitting their data in a given mini-timeslot remain in the *waiting state*. In a conventional PD-NOMA system, multiplexed users have active battery resources, and they transmit at different power levels to exploit the benefits of NOMA. On the other hand, the BNs of the sensor network are passive devices that do not have a capability to actively alter the transmit power level according to their respective channel gains. Hence, we used the different pairs of reflection coefficients for N subregions to implement power-domain NOMA.

A. Training Phase

In the training phase, the reader categorizes all sensors residing in different subregions according to their channel state information (CSI) and a reflection coefficient pair is then assigned to each sensor. Each subregion has a different pair of the reflection coefficient. Similarly, each sensor can also decide which subregion it belongs to. We assume that the reader has the CSI of all sensors, and it is obtained during the training procedure phase. Initially, in the training phase, the reader divides a timeslot of T seconds into L mini-timeslots and broadcasts the RF training signal with a distinct identification (ID) value. Only one sensor can transmit in the assigned mini-slot. Each sensor on hearing its unique ID value from the reader training signal, responds in the next corresponding mini-timeslot to send the information. The reader receiving the information signal from each sensor obtains the CSI of each respective sensor. Once the sensor is selected from a subregion, the microcontroller of that sensor selects impedance pairs accordingly to set the reflection coefficient. We set the reflection coefficient as, $1 \geq \Gamma_1 \geq \Gamma_2 \geq \dots \Gamma_{n-1} \geq \Gamma_n \dots \geq \Gamma_N > 0$, where $n \leq N - 1$ and Γ_n is the reflection coefficient of sensor residing in n -th subregion. The reflection coefficient has great importance in implementing PD-NOMA for the BackCom IoT system and each subregion should satisfy the following conditions to give the best system performance [11]

$$\Gamma_N = \frac{\tau R^{2\alpha}}{\Omega_t}, \quad (5)$$

$$\Gamma_n \geq \max \left\{ \Gamma_{n+1}, \tau \left(\sum_{j=n+1}^N \Gamma_j \frac{R_{n+1}^{2\alpha}}{R_j^{2\alpha}} + \frac{R_{n+1}^{2\alpha}}{\Omega_t} \right) \right\}, n \leq N - 1 \quad (6)$$

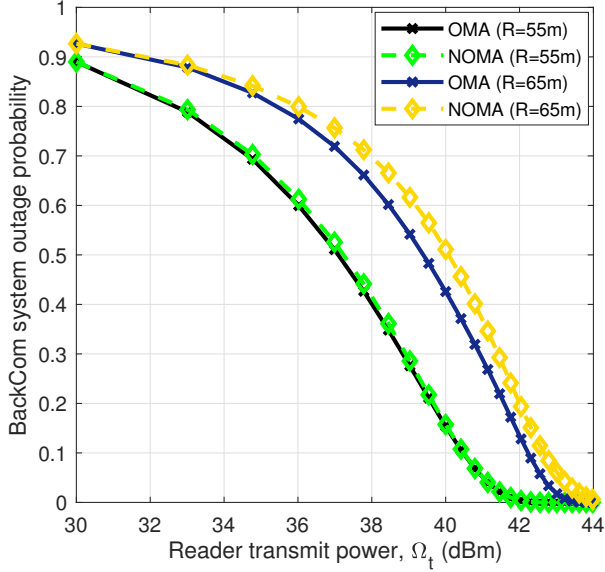
In (5) and (6), τ is the signal-to-interference-plus-noise (SINR) threshold, R_n is the annular radius of n -th subregion from the reader and $R_n \leq R_{n+1}$.

B. Use of Successive Interference Cancellation (SIC)

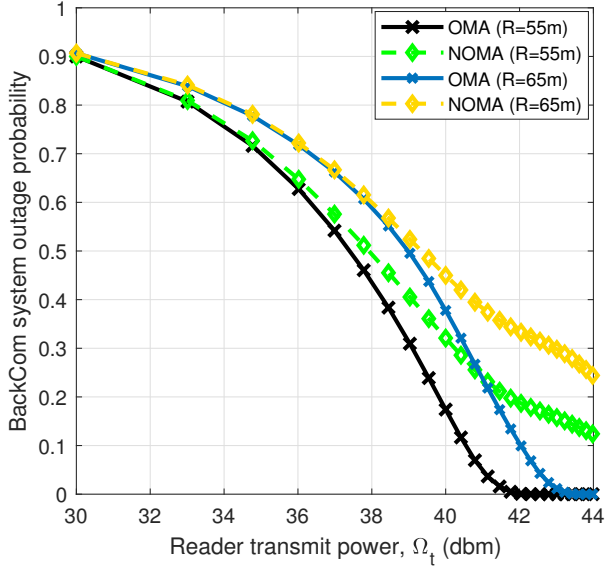
On the reader receiver side, NOMA decoding is performed by using the SIC technique. The received superimposed NOMA signal, y , for n multiplexed sensors at the reader is given by

$$y = \sum_{i=1}^n \sqrt{\Omega_R^i} h_i s^i + m, \quad (7)$$

where s^i represents the information signal, h_i is the channel gain, m denotes the Gaussian noise and Ω_R^i is the received reflected power at reader from the i -th sensor associated with subregion n . The reader performs the SIC operation on received signal, y , and recovers the strongest signal while treating the other weaker signals as interference. If SINR exceeds the threshold, then the signal is assumed to be



(a)



(b)

Fig. 3. NOMA assisted system outage performance for varying Ω_t (a) Scenario 1 (b) Scenario 2

decoded successfully and vice versa. The SINR for any k -th multiplexing sensor during SIC operation is given as

$$\text{SINR}_k = \frac{\sqrt{\Omega_R^k h_k s^k}}{\sigma^2 + \sum_{i=k+1, i \neq k}^n \sqrt{\Omega_r^i h_k s^i}}, \quad (8)$$

where σ^2 is the noise power spectral density.

C. Sensor outage and Throughput

In the decoding process, if the SIR for a sensor is below the threshold, the sensor goes into outage. The decoding

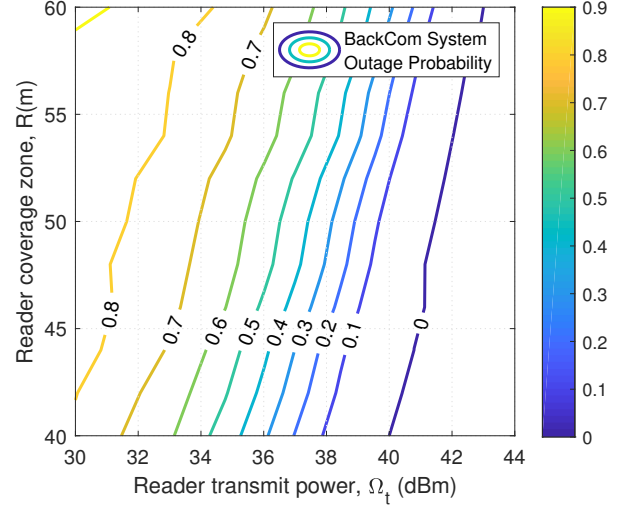


Fig. 4. NOMA assisted system outage performance against a reader transmit power (Ω_t) and reader coverage zone (R).

process stops and it does not continue for remaining weaker sensors. The achievable throughput, \hat{T}_k , for the k -th sensor after successful decoding is given by

$$\hat{T}_k = B \log_2 \left(1 + \frac{\sqrt{\Omega_R^k h_k s^k}}{\sigma^2 + \sum_{i=k+1, i \neq k}^n \sqrt{\Omega_r^i h_k s^i}} \right), \quad (9)$$

where B is the transmission bandwidth.

IV. RESULTS AND SYSTEM PERFORMANCE

We study the performance of the proposed hybrid TDMA-based PD-NOMA scheme in terms of system outage probability and throughput. To benchmark the performance, we select OMA-based TDMA scheme where each sensor is allocated a single dedicated mini-timeslot for transmission. The simulation results are obtained using the Monte-Carlo simulations. For simulations, we consider 300 sensor nodes, i.e., $L = 300$, path-loss exponent, $\gamma = 2.4$, and a unit noise power spectral density $\sigma^2 = 1$. Each BN sends data at the rate of 1 bit/s, i.e., two reflection coefficients are needed to transmit bit 1 and 0. We assume a two subregions case for PD-NOMA, with two sensors multiplexing over a single mini-timeslot. We set the reflection coefficients $\Gamma_1 = 1$ and $\Gamma_2 = 0.75$ for each sensor using OMA scheme, while, $\Gamma_1 = 1$, $\Gamma_2 = 0.75$, $\Gamma_3 = 0.35$ and $\Gamma_4 = 0.1$ for NOMA scheme.

We consider two scenarios for assigning the reflection coefficient pairs in both subregions. In scenario 1, the large coefficient pair (Γ_1 and Γ_2) is assigned to farthest subregion and smallest coefficients (Γ_3 and Γ_4) to the nearest subregion. In scenario 2, coefficients assignments are opposite to that of scenario 1. Fig. 3 reveals the outage performance of both scenarios against the varying transmit power, Ω_t (dBm), of the reader while threshold, τ , is fixed at -45 dBm. From Fig. 3, it is observed that for scenario 1, NOMA gives better performance in terms of system outage for large values of

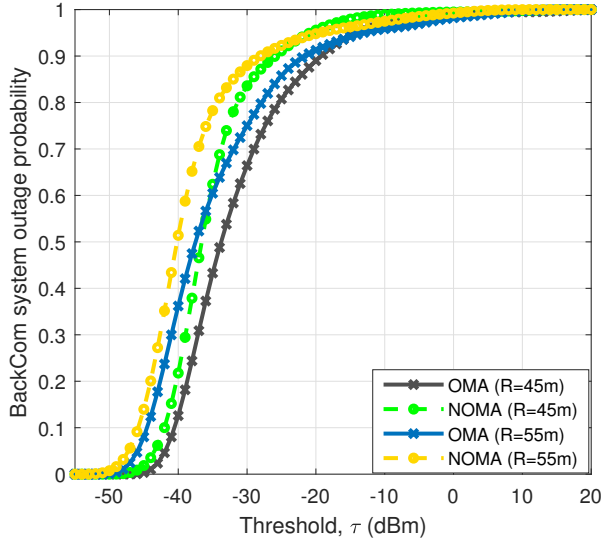


Fig. 5. Outage probability against τ using scenario 1 and $\Omega_t = 36$ dBm.

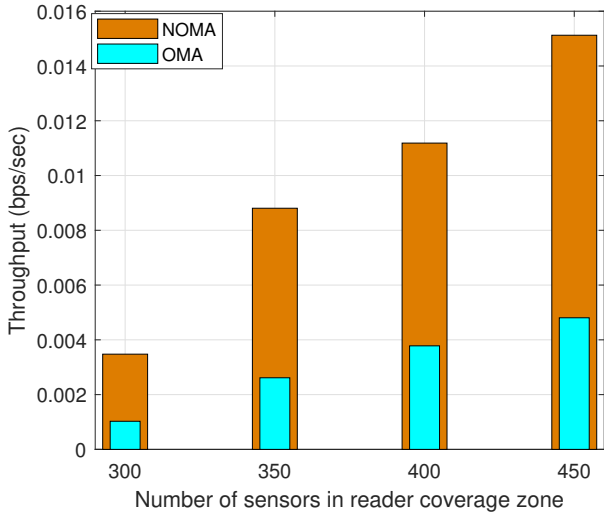


Fig. 6. BackCom system throughput different sensor density in the network

transmit power of the reader. This is because the sensors from the second subregion of the network backscatter higher transmitted power to the reader than the first subregion. Without loss of generality, this decreases the outage event for sensors that belongs to the far subregion in scenario 1 as compared to scenario 2.

For further analysis, we select reflection coefficient assignment scheme as in scenario 1. The contour plot in Fig. 4 shows the system outage with respect to varying both Ω_t and the coverage zone (R) of the reader. It is observed that as the coverage zone increases higher transmit power is needed to maintain the same outage performance. Fig. 5 depicts the outage performance with varying threshold values, τ (dBm). It is observed that for increasing τ , NOMA performance starts degrading. This is due to the fact that at a higher value of τ , outage condition for sensors in subregion 2 becomes strict.

TABLE I
PERCENTAGE IMPROVEMENT IN THE THROUGHPUT FOR HYBRID-NOMA SCHEME COMPARED TO OMA

Number of sensors, L	300	350	400	450
%age increase in throughput	70%	69.5%	69.1%	68.9%

Though this decreases the NOMA performance as compared to OMA, however, NOMA increases the spectrum efficiency of the network by multiplexing all nodes in half of the time duration. Fig. 6 reveals the throughput of the system for different density of sensors. It is observed that using NOMA scheme increases the system throughput significantly as compared to the OMA scheme because of an increase in the spectral efficiency of the system. Table. I displays the percentage increase in throughput of hybrid PD-NOMA scheme with respect to OMA.

V. CONCLUSION

In this paper, we studied a hybrid TDMA-based PD-NOMA multiplexing scheme to increase the spectral efficiency for field-deployed IoT sensors. We evaluated the performance of the BackCom-aided IoT network in term of outage probability and system throughput. The simulation results showed that the proposed PD-NOMA scheme outperforms the conventional TDMA scheme and increases the network capacity to accommodate a large number of sensor nodes. As future work, finding an optimum subregion size to increase the system capacity can be studied.

REFERENCES

- [1] J. Gubbi, R. Buyya, S. Marusic, and M. Palaniswami, "Internet of things (IoT): A vision, architectural elements, and future directions," *Future Generation Computer Systems*, vol. 29, no. 7, pp. 1645–1660, 2013.
- [2] L. Da Xu, W. He, and S. Li, "Internet of things in industries: A survey," *IEEE Trans. Ind. Informat.*, vol. 10, no. 4, pp. 2233–2243, 2014.
- [3] C. Zhu, V. C. Leung, L. Shu, and E. C.-H. Ngai, "Green Internet of things for smart world," *IEEE Access*, vol. 3, pp. 2151–2162, 2015.
- [4] D. Niyato, D. I. Kim, M. Maso, and Z. Han, "Wireless powered communication networks: Research directions and technological approaches," *IEEE W. Commun.*, vol. 24, no. 6, pp. 88–97, 2017.
- [5] N. Van Huynh, D. T. Hoang, X. Lu, D. Niyato, P. Wang, and D. I. Kim, "Ambient backscatter communications: A contemporary survey," *IEEE Commun. Surveys Tut.*, vol. 20, no. 4, pp. 2889–2922, 2018.
- [6] X. Lu, D. Niyato, H. Jiang, D. I. Kim, Y. Xiao, and Z. Han, "Ambient backscatter assisted wireless powered communications," *IEEE W. Commun.*, vol. 25, no. 2, pp. 170–177, 2018.
- [7] K. Han and K. Huang, "Wirelessly powered backscatter communication networks: Modeling, coverage and capacity," *IEEE Trans. on W. Commun.*, vol. 16, no. 4, pp. 2548–2561, 2017.
- [8] S. H. Choi and D. I. Kim, "Backscatter radio communication for wireless powered communication networks," in *Asia-Pacific Conf. on Communications (APCC)*, 2015, pp. 370–374.
- [9] B. Lyu, Z. Yang, G. Gui, and H. Sari, "Optimal time allocation in backscatter assisted wireless powered communication networks," *Sensors*, vol. 17, no. 6, p. 1258, 2017.
- [10] M. N. Jamal, S. A. Hassan, D. N. K. Jayakody, and J. J. Rodrigues, "Efficient nonorthogonal multiple access: Cooperative use of distributed space-time block coding," *IEEE Veh. Technol. Mag.*, vol. 13, no. 4, pp. 70–77, 2018.
- [11] J. Guo, X. Zhou, S. Durrani, and H. Yanikomeroglu, "Design of non-orthogonal multiple access enhanced backscatter communication," *IEEE Trans. W. Commun.*, vol. 17, no. 10, pp. 6837–6852, 2018.
- [12] J. Kimionis and M. M. Tentzeris, "Pulse shaping: The missing piece of backscatter radio and RFID," *IEEE Tran. Microw. Theory Techn.*, vol. 64, no. 12, pp. 4774–4788, 2016.